Progress In Electromagnetics Research M, Vol. 62, 65–77, 2017

A U-Shaped Meandered Slot Antenna for Biomedical Applications

Shikha Sukhija* **and Rakesh K. Sarin**

Abstract—In this paper, a U-shaped microstrip patch antenna with meandered slots is presented. It is designed for biomedical applications to operate at 2.45 GHz. Based on the simulation experience, two designs of the patch are introduced with and without use of meandered slots. The comparative study between these two is also demonstrated. It is observed that the antenna with meandered slots shows good performance with sufficient bandwidth, low losses and is capable of use in biomedical applications. Furthermore, the proposed antenna has small size of $35 * 29 * 1.6$ mm^3, and the size of the ground is only 14% of the overall antenna size. The measured and simulated results show good agreement with each other. The antenna is fabricated on an FR4 substrate, and simulation is carried out on FDTD based Empire XCcel simulator.

1. INTRODUCTION

Rising applications in the field of communication demand many challenging characteristics of a patch antenna. Their naturally favourite properties and inherent advantages such as compactness, ease of fabrication and many other features make microstrip antenna such a prominent device in wireless systems. Many studies on microstrip patch antennas reveal the increasing demand of compactness. Many techniques are available in the literature for miniaturising an antenna such as the usage of a substrate with high permittivity [1] because of the reduced effective wavelength, and operating frequency decreases thus minimising the antenna size. Secondly, by lengthening the path of current flow with the use of meandering structures [2–4], resonant frequency decreases which results in more compact size of the patch antenna. The third technique is the use of shorting pin [5], in which the effective size of the antenna increases, but physical dimensions get reduced as in Planer Inverted F Antennas. The fourth technique is to incorporate vertical stacking to increase the current flow path between two radiating patches [6]. Both meandered and stacked arrangements to reduce the antenna size are presented in [7]. Many other miniaturization techniques are also discussed in [8–12]. A U-shaped microstrip patch antenna is presented in [13]. Meandered slot is used in [14] for better matching characteristics of an antenna. A miniaturized meandered slot antenna is proposed in [15] for its use in biomedical applications.

Emerging applications of the microstrip patch antenna include their needs in biomedical sector too. These growing applications comprise remote health monitoring [16], glucose monitoring [17, 18], self-monitoring [19], digestive monitoring [20], etc. So with the increasing need, the scenario gets changed to the use of patch antenna in biomedical zone. On the other hand, with the rapid increase of diseases, people are now becoming more aware for their health. There are many diseases such as diabetes, cancer, depression, thyroid, tuberculosis and HIV/AIDS in which the human body suddenly gain or lose weight. In these cases, a patient or a person went to the doctor or expert for regular check-up. With the use of patch antenna in a weighing machine, a patient or a person needs not to go to the hospital or gym, and his/her weight can be easily monitored at home as well. The arrangement of such an application is shown in Figure 1.

Received 21 August 2017, Accepted 28 October 2017, Scheduled 8 November 2017

* Corresponding author: Shikha Sukhija (shikhasukhija@yahoo.co.in).
The authors are with the Department of Electronics & Communication, National Institute of Technology, Jalandhar, Punjab 144011, India.

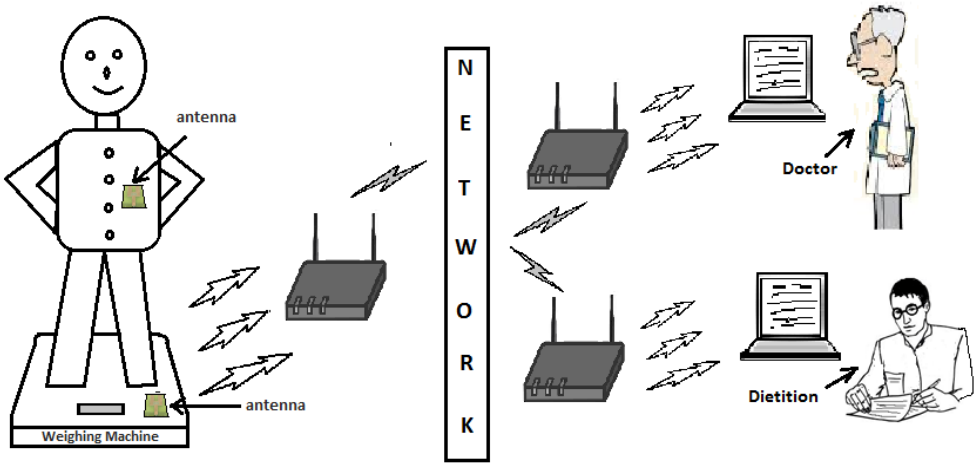

Figure 1. Biomedical application of the proposed antenna.

For the use of antenna in medical applications, frequency bands and power levels are standardized by MICS (Medical Implant Communication Service) band. MICS operates in 402–405 MHz band [21]. Usual frequencies allowed for ISM (Industrial, Scientific and Medical) application are 27 MHz, 433 MHz and 2.45 GHz [22]. Safety issues should be considered when an antenna is implanted inside the human body referring to IEEE C95.1 [23] standardized definitions.

To design an antenna for biomedical applications, one main consideration to be engaged is that the size of the antenna should be small, and it performs good functionality. Microstrip patch antennas offer favourable advantages such as compact size, low cost and easy manufacture. So these antennas are the strong candidates to be used for biomedical applications. In this paper, a U-shaped meandered slot microstrip patch antenna resonating at 2.4 GHz frequency is proposed. Based on [24], a single frequency omnidirectional pattern can be obtained using a U-shaped structure. The proposed antenna works in the ISM (industrial Scientific and Medical) band. Due to its wide bandwidth characteristics, this antenna can also be used in weighing machine for the purpose of remote health monitoring. It implies that if the frequency gets shifted from its original value, it will be within that frequency range because of antenna's wideband features. So, this antenna can be used for remote health monitoring as well as weight monitoring.

2. ANTENNA DESIGN

2.1. Antenna Structure and Design

The proposed antenna shown in Fig. 2 is a U-shaped microstrip patch antenna and consists of two vertical sections and one horizontal section of the patch. The substrate material used for the antenna design is FR4 with dielectric constant of 4.4 and loss tangent of 0.002. The thickness t of the substrate is 1.6 mm, and the overall dimension is $L * W * t\,\text{mm}^3$ $(40 * 33 * 1.6\,\text{mm}^3)$.

Another proposed structure with overall antenna size of $35 * 29 * 1.6\,\text{mm}^3$ is shown in Figure 3. This structure consists of regular meandered slots in a U-shaped patch. A rectangular copper plate along the lower edge of the substrate is used as a ground plane placed opposite to the radiating patch with $29 * 5\,\text{mm}^2$ size. All the dimensions for these proposed structures are described with their values in Table 1.

The zoomed view of the meandered slots structure is shown Figure 4 for better understanding. The slot thickness is 0.5 mm, and length is designed in accordance with the U-shaped structure. The dimension of the single unit of meandered slot is $e * f\,\text{mm}^2$, i.e., $5 * 2.5\,\text{mm}^2$. The meandered parameters and their values are given in Table 2.

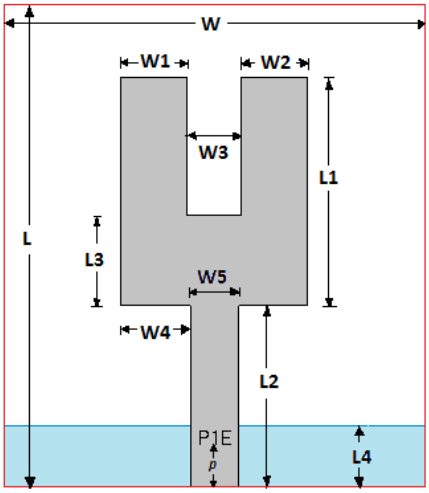

Figure 2. Proposed antenna design.

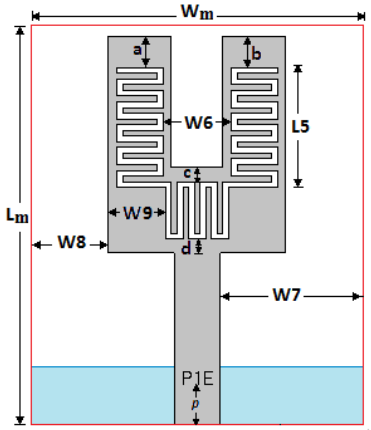

Figure 3. Proposed antenna with meandered slots.

Table 1. Parameters and their values.

Parameters	Values in mm	Parameters	Values in mm
L	40	L_m	35
$L1$	19	$L5$	10.5
$L2$	15	W_m	29
$L3$	7.5	$W6$	6
$L4$	5	$W7$	12.50
W	33	$W8$	6.75
$W1$	5.5	$W9$	5
$W2$	5.5	a	2.75
$W3$	4.5	b	2.75
$W4$	5.75	c	1.25
$W5$	4	d	1.25

2.2. Working Procedure and Design Strategies

The approach was to design a U-shaped patch antenna with sufficient bandwidth and minimum losses to produce the notch at central frequency of 2.45 GHz for bio-medical applications. The strategy for designing this antenna can be summarized as follows:

First Step: A U-shaped patch antenna was designed for 2.45 GHz as the central frequency. Through optimization and calculations, a U-shaped patch antenna is achieved as shown in Figure 2 with parameters given in Table 1. The optimization was supported by fine tuning of the parameters by using FDTD based Empire XCcel simulator [25]. The results are presented later for the purpose of comparison.

Second step: The central meandered slot in the U-shaped patch is introduced with $35 * 29 * 1.6\,\text{mm}^3$ as the overall dimension of the antenna. The optimization in respect of the length of meandered slot was supported by fine tuning of the parameters by FDTD based Empire XCcel simulator. Through optimization, the total length of the central meander became 5.5 mm. The parameters for this antenna are given in Table 1 with their values in mm.

Third step: The left meandered slot in the U-shaped patch was introduced. The optimization in respect of the length of left meandered slot was supported by fine tuning of the parameters by the

Meander parameter	Values in mm
e	5
f	2.5
g	0.5
h	0.5
i	0.5
j	0.5

Table 2. Meander parameters and their values.

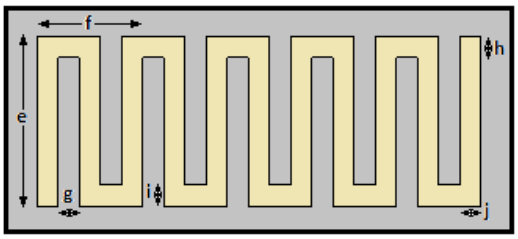

Figure 4. Zoomed view of meandered slots.

above discussed simulator. Using optimization technique, the total length of the left meander became 10.5 mm. The parameters are given in Table 2 with their values in mm.

Fourth step: The right meandered slot was proposed in the U-shaped patch. The optimization in respect of the right meandered slot was supported by fine tuning of the parameters. The total length of the right meandered slot became 10.5 mm which is the same as that obtained in the third step for left slot. Dimensions are presented in Table 2.

Fifth step: After designing these three slots individually, the combinations of central, left and right meandered slots are presented to analyse the performance of the proposed U-shaped meandered slot antenna. The performance of these slots, independently and jointly, are illustrated in the next section.

3. SIMULATIONS AND MEASUREMENT RESULTS

3.1. Optimization of Parameters

Simulation was carried out using the FDTD based Empire XCcel simulator to determine the antenna performance. For the three structures of the meandered slots discussed in the last section, 2^n, i.e., 2^3 combinations can be obtained for analyzing the performance of the proposed antenna. These 8 combinations include no meandered slot, left slot, central slot, right slot, combinations of left and centre, centre and right, left and right, and the combination of all the three slots. The frequency vs. S_{11} parameter graphs for all these combinations individually or jointly with their structures are shown in Figure 5. In the proposed U-shaped antenna, meandered slots are designed to reduce the size of the antenna. As the meandered structure has its own resonant frequency, slots create new edges of the fringing fields which change the resonance frequency of the fundamental mode and generate other modes for new resonant frequency in the form of spikes near fundamental mode. It is observed that symmetric structure results in uniform behaviour of the curve. Contrary to this, the unsymmetrical structures in Figures 5(b) and 5(d) result in nonuniform behaviour of the curve in the form of spikes.

It is also observed that due to the symmetrical structure of the proposed antenna, the performances of left and right slots are exactly same as that shown in Figure 5(b). On the other hand, with the same concept, the performance of joint meandered slots of left-centre and right-centre are also exactly same due to the symmetry property as shown in Figure 5(d). From the above graphs it is concluded that the central frequencies are nearly same for all these structures, and the only difference obtained is in respect of the S_{11} parameters in dB. Figure 5(a) gives the losses up to -23.24 dB, and frequency of operation is 2.392 GHz for the structure shown in Figure 2. Figure 5(f) reveals that -43.72 dB value of S_{11} parameter at 2.478 GHz is obtained using meandered slots for the structure shown in Figure 3. So, it can be concluded that by using meandered slots, the overall antenna size is reduced with enhanced performance. On the other hand, individual left and individual right slots in Figure 5(b) give losses up to -37.07 dB. The 10 dB return loss bandwidth obtained is approximately up to 400 MHz for the proposed antenna. The summarized conclusion of the above results is illustrated in Table 3.

3.1.1. Effect of $\boldsymbol{p}$ *on Performance of the Proposed Antenna*

The distance of the port to the lower edge of the substrate is denoted as p shown in Figure 2 and Figure 3. It is observed that by changing this value, the results overlap each other with the difference of their S_{11} parameter value. Through fine tuning, the optimized position of the port obtained is 0.79 mm.

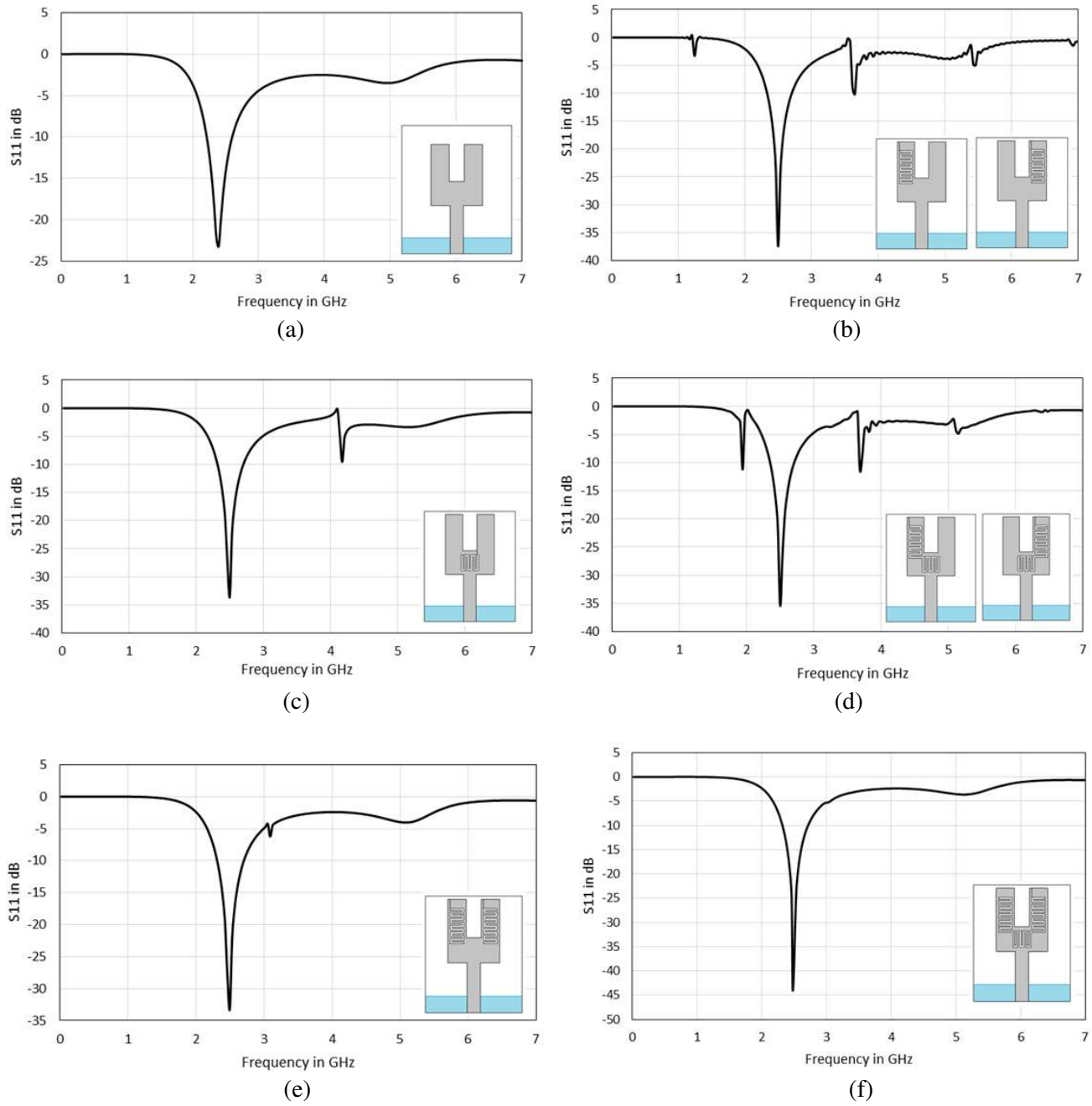

Figure 5. Frequency vs scattering parameter S_{11} for (a) without meandered slot, (b) left and right individual slot, (c) central slot, (d) centre-left and centre-right slots, (e) left-right slot and (f) left-centre-right combined slot.

As this value increases, S_{11} parameter decreases from -43.72 dB to -19.42 dB. The comparison graph for this position at different values is shown in Figure 6. The frequency versus VSWR plot and frequency versus impedance graphs for different values of p are illustrated in Figure 7 and Figure 8, respectively.

3.1.2. Effect of the Length of Ground Plane

The length and width of the ground plane for the proposed antenna are 5 mm and 29 mm, respectively. By fine tuning, the desired central frequency is obtained. Different values of the length of ground plane

Table 3. Performance comparison of 2^3 combination structures of the meandered slots.

Slot Type	f_l (GHz)	f_h (GHz)	f_c (GHz)	Bandwidth obtained (MHz)	S_{11} (dB)
Without meandered slot (Figure 5(a))	2.214	2.598	2.3927	384	−23.22
Left, Right (Figure 5(b))	2.334	2.703	2.4970	369	−37.07
Central (Figure 5(c))	2.316	2.697	2.4988	381	−33.22
Left-Centre, Right-Centre (Figure 5(d))	2.349	2.706	2.4990	357	−35.08
Left-Right (Figure 5(e))	2.313	2.697	2.4989	384	−32.88
Left-Centre-Right (Figure 5(f))	2.319	2.715	2.4782	396	−43.72

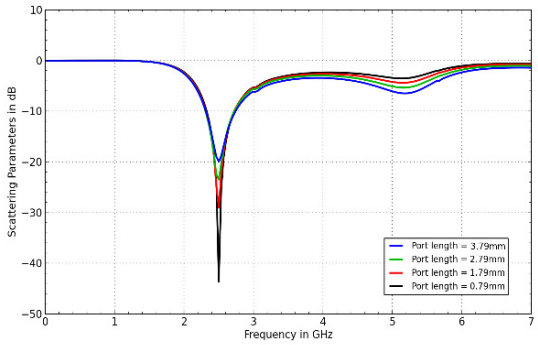

Figure 6. Simulated S_{11} parameter vs. frequency graph for different values of p.

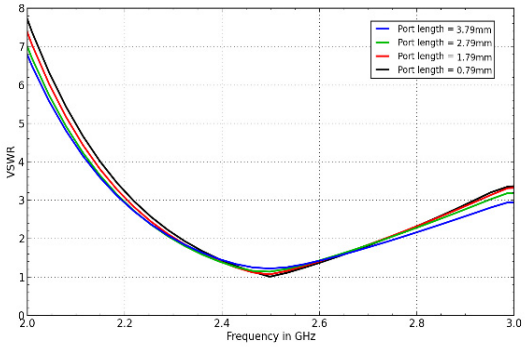

Figure 7. Simulated plot showing VSWR vs. frequency plot for different values of p.

are taken such as 5 mm, 15 mm, 25 mm and 35 mm, and it is perceived that varying this length affects the antenna performance seriously. Figure 9 shows that by changing the ground plane dimensions, the resonant frequency changes its value. As the value of ground length shifts from 5 mm to 15 mm, the behaviour of resonant frequency and S_{11} parameters shift from 2.47 GHz to 3.34 GHz and from −43.72 dB to −19.93 dB, respectively. The frequency versus VSWR plot and frequency versus impedance graphs for different ground plane lengths are illustrated in Figure 10 and Figure 11, respectively.

3.2. Prototyping and Results Discussion

The proposed U-shaped patch antenna with meandered slots structure is fabricated on an FR4 substrate with dielectric constant of 4.4. The image of the fabricated antenna is shown in Figure 12(a). The simulated current distribution is presented in Figures 12(b), (c), (d). It can be visualized that current is flowing uniformly over the patch and is intensive in the U-shaped structure of the antenna. Generally, the operating bandwidth is determined by −10 dB band [26]. The current at lower frequency is generated because of the edges of the patch. Lower, upper and resonant frequencies f is calculated by following equations [27]

$$S_o = S_1 + S_2 + S_3 + S_4 + S_5 + S_6 \tag{1}$$

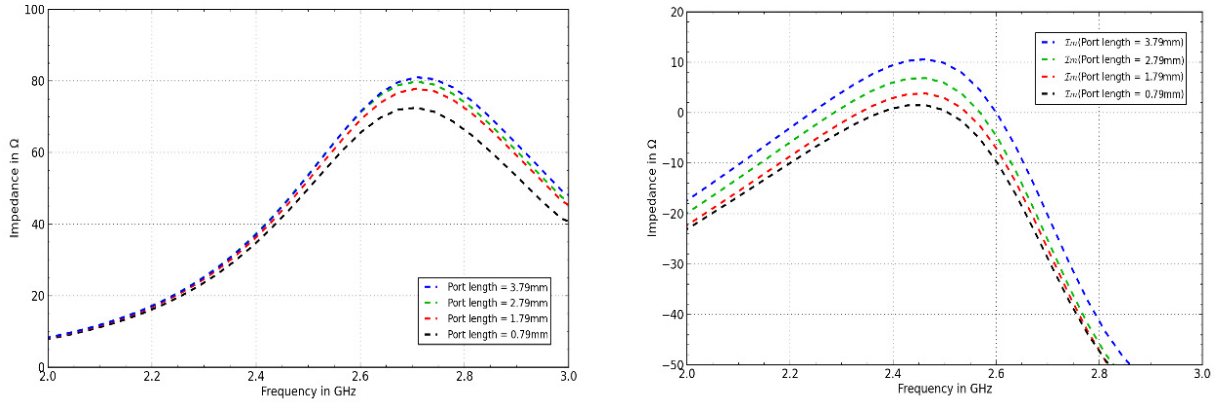

Figure 8. Simulated plots for different values of p, (a) frequency vs. impedance (real-part) and (b) frequency vs. impedance (imaginary part).

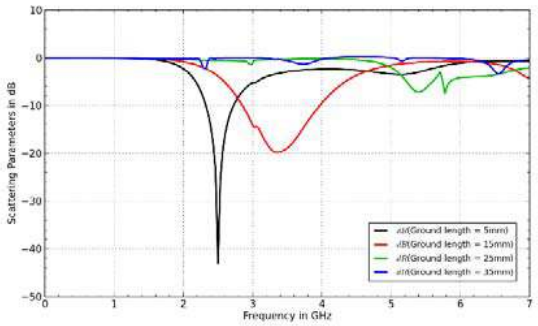

Figure 9. Simulated S_{11} parameter vs. frequency plot for different length of ground plane.

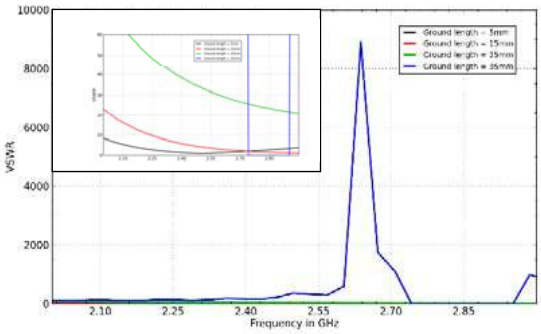

Figure 10. Simulated VSWR plot for different length of ground plane.

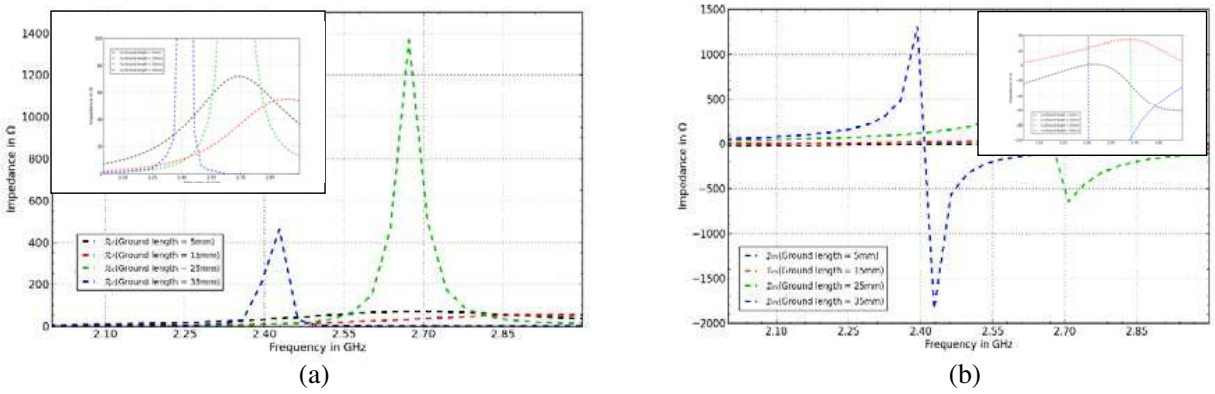

Figure 11. Simulated impedance vs. frequency plots for different length of ground plane, (a) real part and (b) imaginary part.

$$f = \frac{c}{S_o\sqrt{\varepsilon_r}} \tag{2}$$

With the help of above relations, the calculated lower, upper and operating frequencies are obtained as 2.38 GHz, 2.76 GHz and 2.48 GHz, respectively. The simulated S parameters of lower, upper and operating frequencies are included in Table 3.

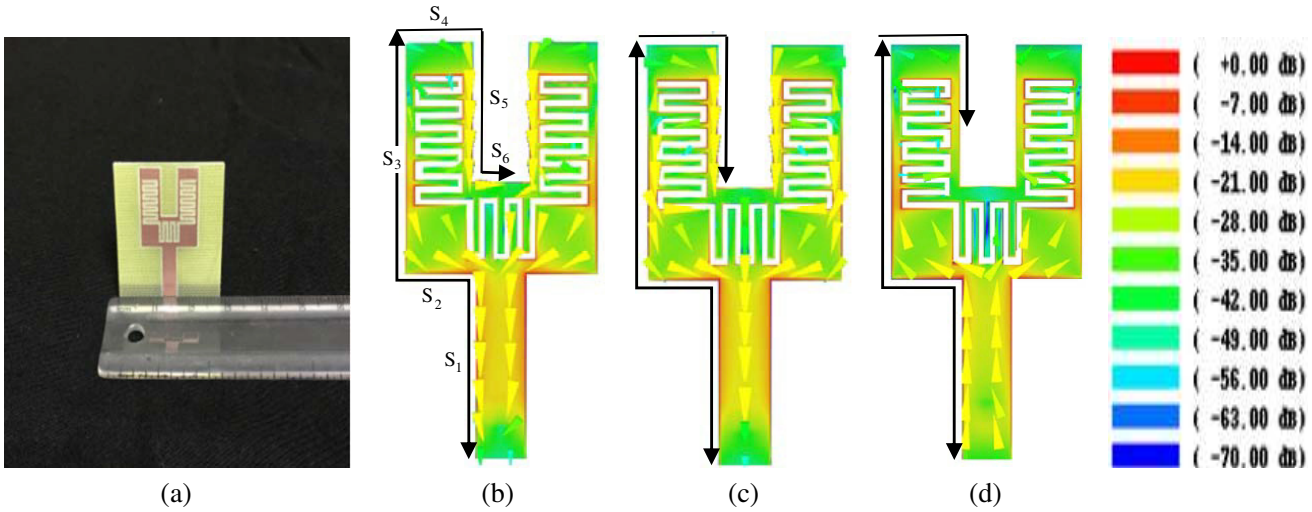

Figure 12. (a) Fabricated antenna photograph, (b) simulated current distribution at 2.31 GHz, (c) simulated current distribution at 2.47 GHz and (d) simulated current distribution at 2.71 GHz.

3.2.1. Equivalent Circuit

An equivalent circuit for the U-shaped antenna is illustrated in Figure 13. This equivalent circuit model contains a parallel RLC circuit in series with reactance. This circuit is used to calculate the input impedance matching at any frequency if the bandwidth, resonant input impedance and resonant frequencies are known [28].

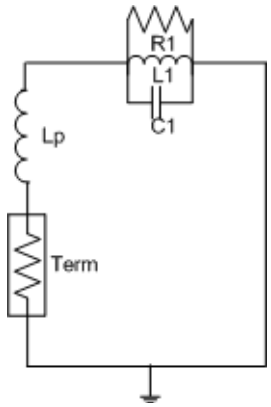

Figure 13. Equivalent circuit model.

It can be concluded from the desired output of the microstrip model that there is direct correlation between the dielectric constant (ε_r), substrate height (h), and the feed width (W_f) with the impedance of the antenna. In RLC tank circuit, if the value of $R1$ is 50 Ω, then at each operating frequency, the values of $C1$, $L1$ and L_p are given as:

$$C1 = \frac{2W_f\varepsilon_r}{Lh\omega_0^2}, \quad L1 = \frac{1}{C1\omega_0^2} \quad \text{and} \quad L_p = \frac{W_f L1}{L}$$

where L_p is a series inductor due to coaxial feed probe, and L is the length of the proposed antenna. The calculated values for $C1$, $L1$ and L_p, according to the aforementioned equations, are 5.18 pF, 0.79 nH and 0.18 nH, respectively.

3.2.2. Measurement Results

The performance of the proposed antenna structure is analyzed in terms of S_{11} parameters. SMA connector of the antenna to be tested is connected to a co-axial cable of a vector network analyzer. One port calibration is performed using calibration standards such as short, open and load. The S_{11} parameter vs. frequency graph is plotted for the proposed antenna as simulated by Finite Difference Time Domain (FDTD) based Empire XCcel simulator together with measurement using VNA. Due to the useful advantage of the proposed antenna, the behaviour of the antenna is measured by using chicken. As the dielectric properties of chicken and human muscle are almost same [29], this model was developed to provide real environment for the antenna applicable to biomedical applications [30].

The tissue thickness for three layers, i.e., skin/fat/muscle [31] and dielectric properties [32] are tabulated in Table 4 and Table 5, respectively. As a matter of fact, there is no significant change in the matching characteristics by incorporating muscle model. It only changes the dielectric constant by 20% and resonant frequency by approximately 4% [33].

Table 4. Human tissues and their thickness for the proposed antenna [31].

Human tissue	Thickness in mm
Skin	4
Fat	4
Antenna substrate	1.6
Muscle	8

Table 5. Dielectric properties of human tissues [32].

Tissue	Permittivity ε_r	Conductivity σ (S/m)
Muscle	52.7	1.73
Skin	38	1.46
Fat	5.28	0.10
Bone	18.54	0.80

The combined simulated and measured S_{11} parameter performances of this antenna are illustrated in Figure 14. It can be illustrated that the antenna resonates at 2.478 GHz and exhibits 396 MHz simulation bandwidth in free space while the antenna in muscle environment resonates at 2.114 GHz frequency and has simulation bandwidth of 209.4 MHz. On the other hand, it can also be seen that the proposed antenna measurement in free space displays the bandwidth of 468 MHz at 2.4532 GHz, and in chicken environment it exhibits bandwidth of 279.2 MHz at 2.1489 GHz. Due to its measured wideband characteristics, this antenna can also be used in weighing machine for the purpose of remote health monitoring. This implies that if the frequency gets shifted from its original value due to circuitry effect, it will be within that frequency range because of antenna's wideband features. Table 6 exhibits the comparison of the proposed antenna with some reported antennas at 2.45 GHz.

Table 6. Comparison of different antennas at 2.45 GHz.

Reference	S_{11} parameter	Size (mm^2)	Substrate used
[34]	-31	35×40	PET substrate
[35]	-22	50.33×32	FR4 and Macor
[36]	-36.66	41.5×29	FR4
[37]	-14.2	50×16	jean
Proposed	-43.72	35×29	FR4

The simulated and measured radiation patterns for the proposed antenna are presented in Figure 15. The patterns are plotted at 2.45 GHz frequency. These radiation pattern measurements for rf and microwave range frequencies have been performed using an anechoic chamber. The figure shows the radiation patterns for both E-plane and H-plane. For H-plane, the co-polar component shows monotonous behaviour as expected, and the measured patterns are also showing similar characteristics except at some points owing to the existence of parasitic effect in SMA connector. On the other hand, the co-polar component in E-plane has a well-known shape like figure eight (8) as expected. Measured

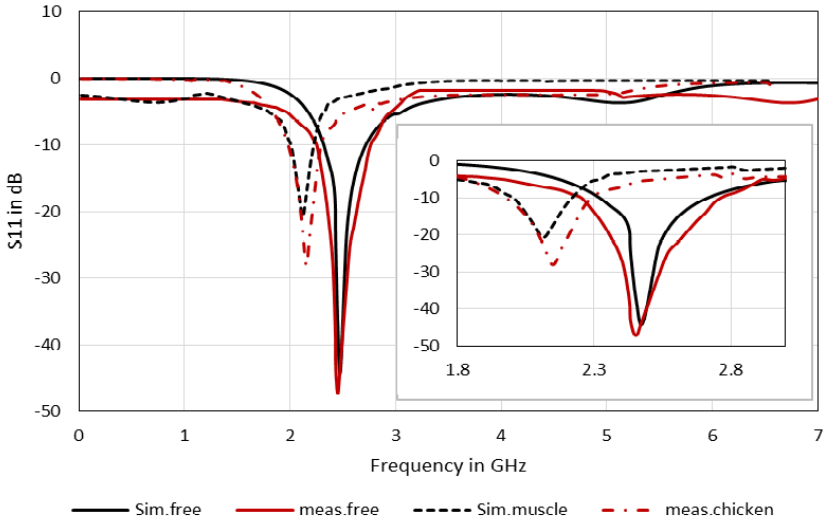

Figure 14. Simulated vs. measured S_{11} parameter graph.

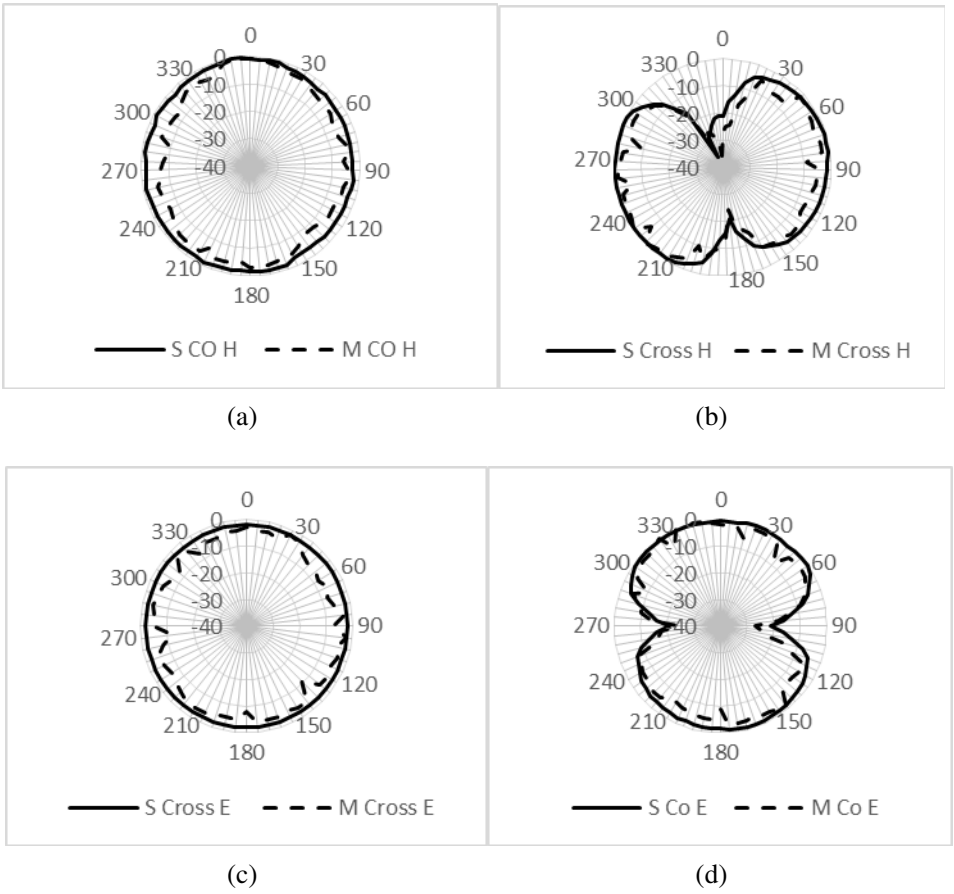

(a) (b)

(c) (d)

Figure 15. Simulated vs. measured co-polar and cross polar plots for the proposed antenna at 2.45 GHz.

results show good resemblance with simulated results. Some deviation occurs due to the SMA connector and feeding connector, but these are still within the acceptable limits. It can be observed that at resonant frequency, the pattern obtained is almost omnidirectional.

The antenna transfer function was obtained using two identical antennas to calculate the transmission coefficient $S_{21}(\omega)$, for the two identical antennas separated by a distance r between their apertures. The distance was chosen to satisfy the general far-field requirement $r \geq 2D^2/\lambda$ where D is the maximum dimension of the aperture of the antenna [38]. The antenna transfer function was then calculated using Eq. (3), and the frequency domain gains are calculated using Equation (4)

$$\bar{H}(\omega)_{ant} = \sqrt{\frac{2\pi rc}{j\omega}\bar{S}_{21}(\omega)e^{+j\omega r/c}} \tag{3}$$

$$G(\omega)_{ant} = \frac{4\pi f^2}{c^2}\left|\bar{H}(\omega)_{ant}\right|^2 \tag{4}$$

The S_{21} of the proposed antenna gain is shown in Figure 16.

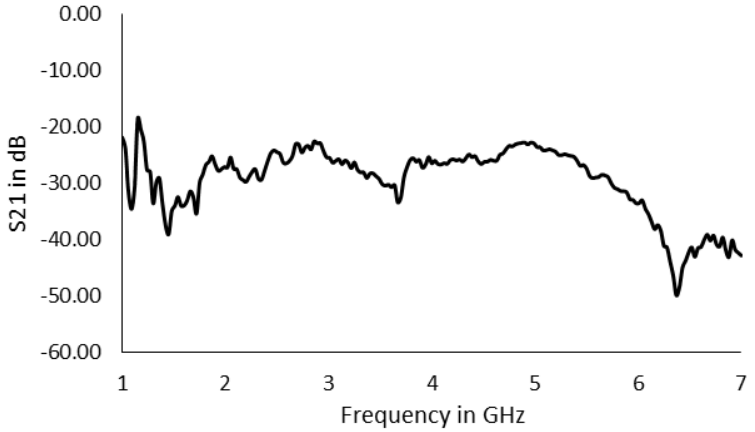

Figure 16. Measured S_{21} vs. frequency graph for the proposed antenna.

4. CONCLUSION

This paper reports a design of U-shaped patch antenna with meandered slots for ISM band application and explains the comparison between experimental results of the proposed antenna in free space and muscle model. Due to its wide bandwidth features, this antenna can be used for remote health monitoring system. The measured and simulated results give similar response. Its compactness, good frequency vs. losses response, radiation pattern will definitely help this designed antenna to be an effective candidate for biomedical applications. The characterization of the proposed antenna in weighing machine will be of great interest. Future scope also includes more reduction in size and SAR calculation of the proposed antenna.

ACKNOWLEDGMENT

The authors would like to thank Care Lab at Indian Institute of Technology, Delhi for measurement of radiation patterns and Dr. Nitesh Kashyap for providing timely help and support.

REFERENCES

1. Kim, J. and Y. Rahmat-Samii, "Implanted antennas inside a human body: Simulations, designs, and characterizations," *IEEE Transactions on Microwave Theory and Techniques*, Vol. 52, No. 8, 1934–1943, Aug. 2004.
2. Kim, J.-M., J.-G. Yook, W.-Y. Song, Y.-J. Yoon, J.-Y. Park, and H.-K. Park, "Compact meander-type slot antennas," *IEEE Antennas and Propagation Society International Symposium, 2001*, Vol. 2, 724–727, Jul. 8–13, 2001.

3. Kiourti, A. and K. S. Nikita, "Miniature scalp-implantable antennas for telemetry in the MICS and ISM bands: Design, safety considerations and link budget analysis," *IEEE Transactions on Antennas and Propagation*, Vol. 60, No. 8, 3568–3575, Aug. 2012.
4. Kiourti and K. S. Nikita, "Meandered versus spiral novel miniature pifas implanted in the human head: Tuning and performance," *Proceedings of the 2nd ICST International Conference on Wireless Mobile Communication and Healthcare (MobiHealth 2012)*, Kos Island, Greece, Oct. 2011.
5. Soontornpipit, P., C. M. Furse, and Y. C. Chung, "Design of implantable microstrip antenna for communication with medical implants," *IEEE Transactions on Microwave Theory and Techniques*, Vol. 52, No. 8, 1944–1951, Aug. 2004.
6. Kiourti, A., M. Christopoulou, and K. S. Nikita, "Performance of a novel miniature antenna implanted in the human head for wireless biotelemetry," *IEEE International Symposium on Antennas and Propagation*, Spokane, Washington, Jul. 2011.
7. Jain, L., R. Singh, S. Rawat, and K. Ray, "Stacked arrangement of meandered patches for biomedical applications," *Int. J. Syst. Assur. Eng. Manag.*, 1–8, 2016.
8. Soontornpipit, P., C. M. Furse, and Y. C. Chung, "Miniaturized biocompatible microstrip antenna using genetic algorithm," *IEEE Transactions on Antennas and Propagation*, Vol. 53, No. 6, 1939–1945, Jun. 2005.
9. Huang, F. J., C. M. Lee, C. L. Chang, L. K. Chen, T. C. Yo, and C. H. Luo, "Rectenna application of miniaturized implantable antenna design for triple-band biotelemetry communication," *IEEE Transactions on Antennas and Propagation*, Vol. 59, No. 7, 2646–2653, Jul. 2011.
10. Liu, W. C., F. M. Yeh, and M. Ghavami, "Miniaturized implantable broadband antenna for biotelemetry communication," *Microwave and Optical Technology Letters*, Vol. 50, No. 9, 2407–2409, Sep. 2008.
11. Liu, W. C., S. H. Chen, and C. M. Wu, "Bandwidth enhancement and size reduction of an implantable PIFA antenna for biotelemetry devices," *Microwave and Optical Technology Letters*, Vol. 51, No. 3, 755–757, Mar. 2009.
12. Sukhija, S. and R. K. Sarin, "Low-profile patch antennas for biomedical and wireless applications," *J. Comput. Electron.*, Vol. 16, No. 2, 354–368, Jun. 2017.
13. Koohestani, M. and M. Golpour, "U-shaped microstrip patch antenna with novel parasitic tuning stubs for ultra-wideband applications," *IET Microwaves, Antennas & Propagation*, Vol. 4, No. 7, 938–946, Jul. 2010.
14. Kaya, A., "Meandered slot and slit loaded compact microstrip antenna with integrated impedance tuning network," *Progress In Electromagnetics Research B*, Vol. 1, 219–235, 2008.
15. Xu, L.-J., Y.-X. Guo, and W. Wu, "Miniaturised slot antenna for biomedical applications," *Electronics Letters*, Vol. 49, No. 17, 1060–1061, Aug. 15, 2013.
16. Hall, P. S. and Y. Hao, *Antennas and Propagation for Body-centric Communications*, Artech House, London and Boston, 2006.
17. Karacolak, T., A. Z. Hood, and E. Topsakal, "Design of a dual-band implantable antenna and development of skin mimicking gels for continuous glucose monitoring," *IEEE Transactions on Microwave Theory and Techniques*, Vol. 56, No. 4, 1001–1008, Apr. 2008.
18. Beach, R. D., F. V. Kuster, and F. Moussy, "Subminiature implantable potentiostat and modified commercial telemetry device for remote glucose monitoring," *IEEE Transactions on Instrumentation and Measurement*, Vol. 48, No. 6, 1239–1245, Dec. 1999.
19. Tak, J., K. Kwon, and J. Choi, "Design of a dual band repeater antenna for medical self-monitoring applications," 2013 *IEEE Antennas and Propagation Society International Symposium (APSURSI)*, 2091–2092, July 7–13, 2013.
20. Malika, T., K. Abdennaceur, A. Rahma, and A. Frederic, "Miniaturized on-body patch antenna for 430 MHz wireless digestive monitoring system," *2014 IEEE Workshop on Biometric Measurements and Systems for Security and Medical Applications (BIOMS) Proceedings*, 57–60, Oct. 17, 2014.
21. Medical Implant Communication Service (MICS) federal register, Rules reg., Vol. 64, No. 240, Dec. 1999.

22. Smith, E. K., "Radiowave propagation in ITU-R," *IEEE Magazine in Antennas and Propagation*, Vol. 41, No. 1, 118–119, Feb. 1999.
23. IEEE Standard for safety levels with respect to human exposure to radio frequency electromagnetic fields, 3 kHz to 300 GHz, IEEE Standard C95.1-1999, 1999.
24. Nezhad, S. M. A., G. Dadashzadeh, and A. Foudazi, "A tunable dual band notch on a UWB printed slot monopole antenna by using open circuit stubs," *Microwave and Optical Technology Letters*, Vol. 53, No. 8, 1931–1935, 2011.
25. User and Reference Manual for the 3D EM Time Domain Simulator Empire XCcel, ver. 5.5, IMST GmbH, 2012, [online], available: http://www.empire.de/.
26. Balanis, C. A., *Antenna Theory Analysis and Design*, 3rd Edition, John Wiley, 2005.
27. Shukla, B. K., N. Kashyap, and R. K. Baghel, "Circular slotted elliptical patch antenna with elliptical notch in ground," *Progress In Electromagnetics Research C*, Vol. 74, 181–189, 2017.
28. Sayidmarie, K. H. and L. S. Yahya, "Modeling of dual-band crescent-shape monopole antenna for WLAN applications," *International Journal of Electromagnetics and Applications*, Vol. 4, No. 2, 31–39, 2014.
29. Tran, V. N. and S. S. Stuchly, "Dielectric properties of beef, beef liver, chicken and salmon at frequencies from 100 to 2500 MHz," *Journal of Microwave Power and Electromagnetic Energy*, Vol. 22, 29–33, 1987.
30. Ashok Kumar, S. and T. Shanmuganantham, "Analysis and design of implantable Z-monopole antennas at 2.45 GHz ISM band for biomedical applications," *Microwave and Optical Technology Letters*, Vol. 57, No. 2, 468–473, 2015.
31. Duan, Z., Y. X. Guo, R. F. Xue, M. Je, and D. L. Kwong, "Differentially fed dual-band implantable antenna for biomedical applications," *IEEE Transactions on Antennas and Propagation*, Vol. 60, No. 12, 5587–5595, Dec. 2012.
32. Gabriel, S., R. W. Lau, and C. Gabriel, "The dielectric properties of biological tissues: III. Parametric models for the dielectric spectrum of tissues," *Physics in Medicine and Biology*, Vol. 41, 2271–2293, Nov. 1996.
33. Lee, C. M., T. C. Yo, F. J. Huand, and C. H. Luo, "Bandwidth enhancement of planar inverted-F antenna for implantable biotelemetry," *Microwave and Optical Technology Letters*, Vol. 51, 749–752, Mar. 2009.
34. Guo, X., Y. Hang, Z. Xie, C. Wu, L. Gao, and C. Liu, "Flexible and wearable 2.45 GHz CPW-fed antenna using inkjet-printing of silver nanoparticles on pet substrate," *Microwave and Optical Technology Letters*, Vol. 59, No. 1, 204–208, 2017.
35. Salim, M. and A. Pourziad, "A novel reconfigurable spiral-shaped monopole antenna for biomedical applications," *Progress In Electromagnetics Research Letters*, Vol. 57, 79–84, 2015.
36. Sukhija, S. and R. K. Sarin, "Design and performance of two-sleeve low profile antenna for biomedical applications," *Journal of Electrical Systems and Information Technology*, Vol. 4, No. 1, 49–61, 2017.
37. Gil, I. and R. Fernández-García, "Wearable PIFA antenna implemented on jean substrate for wireless body area network," *Journal of Electromagnetic Waves and Applications*, Vol. 31, Nos. 11–12, 1194–1204, 2017.
38. Nel, M., J. Joubert, and J. W. Odendaal, "The measurement of complex antenna transfer functions for ultra-wideband antennas in a compact range [measurements corner]," *IEEE Antennas and Propagation Magazine*, Vol. 56, No. 6, 163–170, 2014.